Available online at www.sciencedirect.com
ScienceDirect
European Journal of Mechanics B/Fluids 27 (2008) 643–664

The reservoir technique: a way to make Godunov-type schemes zero or very low diffuse. Application to Colella–Glaz solver

François Alouges [a], Florian De Vuyst [b], Gérard Le Coq [c], Emmanuel Lorin [d,e,*]

[a] *Laboratoire de Mathématiques, Université d'Orsay, 91405 Orsay, France*
[b] *Laboratoire MAS, Ecole Centrale de Paris, Grande voie des vignes, 92295 Chatenay-Malabry, France*
[c] *Centre de Mathématiques et de Leurs Applications, ENS de Cachan, 61, avenue du président Wilson, 94235 Cachan cedex, France*
[d] *Centre de Recherches Mathématiques, Université de Montréal, 2920 Chemin de la Tour, H3T 1J4, Canada*
[e] *University of Ontario Institute of Technology, 2000 Simcoe Street North, L1H 7Y4, Oshawa, Canada*

Received 7 February 2006; received in revised form 28 July 2006; accepted 22 January 2008

Available online 3 February 2008

Abstract

Although it is commonly thought that first order schemes are not accurate enough to approximate nonlinear hyperbolic problems, we here explore a conservative time integration with global time steps but local updates (see [F. Alouges, F. De Vuyst, G. Le Coq, E. Lorin, Un procédé de réduction de la diffusion numérique des schémas à différence de flux d'ordre un pour les systèmes hyperboliques non linéaires, C. R. Math. Acad. Sci. Paris, Ser. I 335 (7) (2002) 627–632. [1]]; [F. Alouges, F. De Vuyst, G. Le Coq, E. Lorin, The reservoir scheme for systems of conservation laws, in: Finite Volumes for Complex Applications, III, Porquerolles, 2002, Lab. Anal. Topol. Probab. CNRS, Marseille, 2002, pp. 247–254 (electronic). [2]]). This overall conservative method can be interpreted as a system of reservoirs at cell interfaces that fill up and empty when local CFL conditions are reached. For Euler equations, particularly good results are obtained when one uses this technique together with the Riemann solver proposed by Colella and Glaz.
© 2008 Published by Elsevier Masson SAS.

Keywords: Finite volume scheme; Numerical diffusion; Hyperbolic systems of conservation laws

1. Introduction

Today's contributions on the design of numerical schemes to approximate solutions of hyperbolic problems mainly deal with high order of accuracy. This task is particularly difficult since solutions of such systems likely present singularities, shock waves, contact discontinuities, which are difficult to catch with classical numerical methods. Research still aims at achieving high order of accuracy while preserving properties of stability, conservation, discrete entropy inequalities, etc., although large advances have been performed on this subject (spectral methods [3], approximation using wavelets [4], MUSCL, ENO and WENO constructions [5,6]). We can also cite [7,8], and more recently [9–12]. More particularly, Després, Lagoutière proposed in [13,10], an antidiffusive approach based on an Ultra Bee scheme

* Corresponding author.
E-mail address: lorin@crm.umontreal.ca (E. Lorin).

0997-7546/$ – see front matter © 2008 Published by Elsevier Masson SAS.
doi:10.1016/j.euromechflu.2008.01.001

with splitting in multiD. For particular initial data, they were able in 2-D, to prove the exact convection for a constant velocity on regular grids. Bouchut [14] proposed an entropic version of the Després–Lagoutière scheme for monotone scalar conservation laws. Xu and Shu have proposed in [15] a WENO version of the first order Després–Lagoutière anti-diffusive flux corrections. Actually most common high order schemes are not completely satisfactory. First, the local precision is generally lost when complex unstructured meshes with irregular elements are used. This is due to interpolation methods losing their high order of accuracy near "irregular" volumes. Secondly, near strong gradient regions, usual slope limiting methods fall down to first order. Moreover, an error analysis that uses residual estimates of Taylor expansions have no meaning for discontinuities. In the limit, a shock capturing method with the ability of capturing discontinuities on very few points would avoid many problems encountered with existing methods such as material fronts with no mixing process, spurious waves and oscillations generated by linear waves [16], etc. It could also raise theoretical difficulties that are inextricable today such as, for example: proofs of convergence to weak solutions of nonconservative schemes [17].

On the other hand, from a practical point of view, first order schemes are still very useful because of their simplicity and theoretical properties. It is usually quite easy to prove BV or L^∞ stability results, in the framework of nonlinear hyperbolic systems of conservation laws, and discrete entropy properties are fulfilled. In industrial and concrete applications, first order schemes – although easy to implement – are known to produce a too large amount of numerical dissipation, making them bad candidates for wave capture (shocks, boundary layers) or physical quantity assessments and phenomenon modeling (heat flux near walls, turbulence, reactive layers, shock layer for two-phase flows, etc.).

However, in the simple case of pure one-dimensional advection problems with constant propagation velocity a, the upwind scheme can lead to very accurate results when the time step is calibrated according to the Courant–Friedrich–Lewy criterion, also called CFL condition.

Let us consider the advection problem, with $a > 0$:

$$\begin{cases} \partial_t u + a\partial_x u = 0, \quad x \in \mathbb{R},\ t \geqslant 0, \\ u(0,x) = u_0(x) \in BV(\mathbb{R}). \end{cases} \tag{1}$$

We consider an uniform grid of constant mesh size Δx and time step Δt. The solution u of (1) is approximated by the sequence

$$u_j^n \sim u(j\Delta x, n\Delta t), \quad \forall j \in \mathbb{Z},\ \forall n \in \mathbb{N}$$

computed from the initial value $(u_j^0)_{j\in\mathbb{Z}}$, and the conservative explicit first order upwind scheme

$$\begin{cases} \forall n \geqslant 0, \forall j \in \mathbb{Z}, \quad u_j^{n+1} = u_j^n - a\dfrac{\Delta t}{\Delta x}(u_j^n - u_{j-1}^n), \\ u_j^0 = u_0(j\Delta x). \end{cases}$$

It is well known that this scheme is stable under the CFL condition:

$$\lambda = a\frac{\Delta t}{\Delta x} \in]0, 1],$$

so that taking $\Delta t = \Delta x/a$ ($\lambda = 1$) leads to

$$u_j^{n+1} = u_{j-1}^n,$$

which describes the exact propagation of the solution at the discrete level. We generally observe that $u_j^{n+1} = (1-\lambda)u_{j-1}^n + \lambda u_j^n$ is a convex combination of u_{j-1}^n and u_j^n and therefore a mixing of both states if $\lambda < 1$. This mixing may be seen as a loss of information excepted when $\lambda = 1$. Indeed, taking any strictly convex entropy S leads to

$$S(u_j^{n+1}) \leqslant (1-\lambda)S(u_{j-1}^n) + \lambda S(u_j^n)$$

and the inequality is strict if $\lambda < 1$. Hence any total entropy $\sum_j S(u_j^n)$ decreases in time if $\lambda < 1$. For $\lambda = 1$ the entropy is conserved which is what we expect on the exact solution.

Unfortunately, taking $\Delta t = \Delta x/a$ is too restrictive with more general equations (if a is not constant in space for example). At best, the time step Δt may be adapted to ensure the stability condition $\lambda \leqslant 1$ everywhere, which

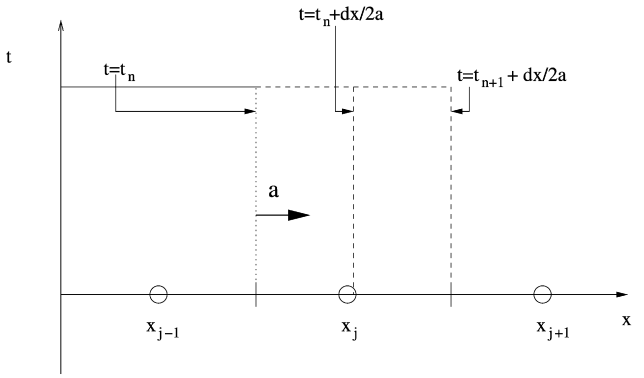

Fig. 1. Reservoir technique principle in (x, u)-space.

involves regions in space where $\lambda < 1$. In these regions, the scheme solves (up to a second order error term) the following equation

$$\partial_t u + a\partial_x u = \frac{\Delta x}{2}(1-\lambda)\partial_x(a\partial_x u)$$

and therefore a smoothing of the solution (due to the viscous term) will occur. From these observations, keeping sharp interfaces in the computation requires to avoid as most as possible this numerical viscosity effect. We therefore design our numerical scheme to behave as if λ were equal to one (or any user prescribed value) although the time step (constrained by another phenomenon elsewhere in the simulation) is smaller than $\Delta t^* = \Delta x/a$. The idea is to freeze the solution while the local cumulated time step (see details below) is not equal to Δt^*. For example, if $\Delta t = \Delta t^*/2$, it is easily seen that one obtains the correct solution by waiting two time steps before updating the solution.

Let us generalize this idea in the case of the advection equation with nonconstant speed

$$\partial_t u + a(x)\partial_x u = 0.$$

The speed $a(x) > 0$ is discretized with one value per interface $a_{j-1/2} = a((j-1/2)\Delta x)$. We introduce a sequence of time steps Δt_n (to be determined later), $R^n_{j-1/2}$ the reservoir associated to the interface $j-1/2$ at time t_n (initialized to $R^0_{j-1/2} = 0$) and $c^n_{j-1/2}$ a positive real CFL counter (also initialized to $c^0_{j-1/2} = 0$). At each time step, we fill up $R^n_{j-1/2}$ with the local current numerical flux difference multiplied by $\Delta t_n/\Delta x$ (see Fig. 1). Then we update the solution and reinitialize both the reservoir and the counter only when the local CFL counter reaches 1. In other words these three quantities (solution, counter and reservoir) are updated in the following manner:

$$\begin{pmatrix} u^{n+1}_j \\ c^{n+1}_{j-1/2} \\ R^{n+1}_{j-1/2} \end{pmatrix} = \begin{cases} \begin{pmatrix} u^n_j \\ c^n_{j-1/2} + \dfrac{a_{j-1/2}\Delta t_n}{\Delta x} \\ R^n_{j-1/2} - a_{j-1/2}\dfrac{\Delta t_n}{\Delta x}(u^n_j - u^n_{j-1}) \end{pmatrix}, & \text{if } c^n_{j-1/2} + a_{j-1/2}\dfrac{\Delta t_n}{\Delta x} < 1, \\ \begin{pmatrix} u^n_j + R^n_{j-1/2} - a_{j-1/2}\dfrac{\Delta t_n}{\Delta x}(u^n_j - u^n_{j-1}) \\ 0 \\ 0 \end{pmatrix}, & \text{if } c^n_{j-1/2} + a_{j-1/2}\dfrac{\Delta t_n}{\Delta x} = 1. \end{cases}$$

Notice that for classical stability reasons, Δt_n must satisfy

$$\sup_j \left(c^n_{j-1/2} + a_{j-1/2}\frac{\Delta t_n}{\Delta x} \right) \leqslant 1,$$

and be as big as possible to shorten the computation time. This leads to the choice

$$\Delta t_n = \min_j \left((1 - c^n_{j-1/2})\frac{\Delta x}{a_{j-1/2}} \right).$$

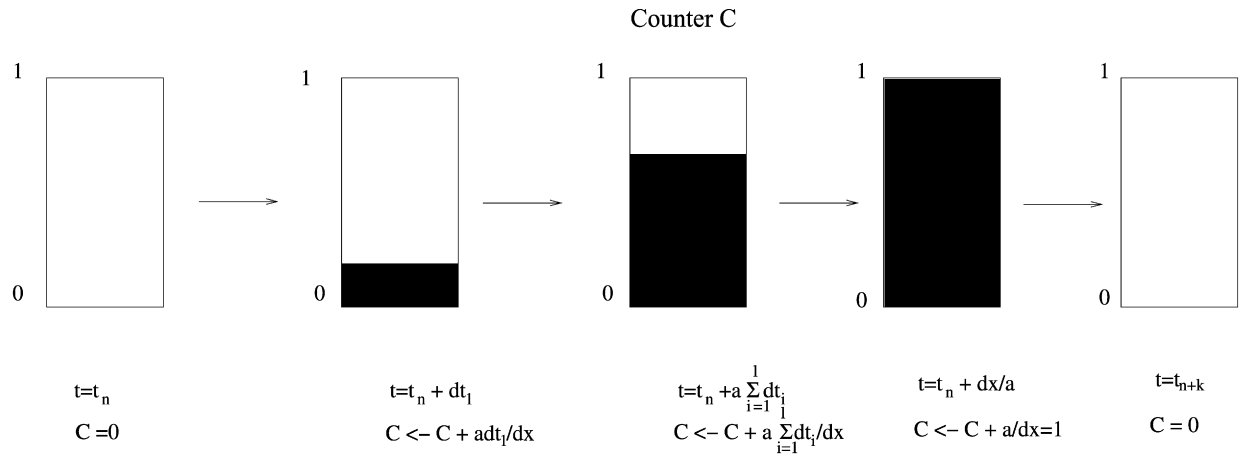

Fig. 2. Counters: an interpretation of the dynamics of computational cells by counters that fill up then empty-up once they are equal to 1.

In this scheme, reservoirs fill up until the local CFL counter is equal to one. They are then emptied in the current cell yielding a CFL $= 1$ like behavior. Note that this process is stable and consistent with the original equation (1) since time steps are smaller than the ones of the CFL $= 1$ scheme. Remark also that in all the above expressions, we could choose to update the solution when counters reach any value less than 1. It may even be taken depending on j as far as values smaller than 1 are chosen. In that case, one introduces some numerical dissipation that regularizes the solution. This possibility, although not desirable, will be used in our numerical results in the case of a non-highly precise Riemann solver. Moreover in general, CFL counters do not reach arithmetically exactly 1 (in particular, because ratios between velocities and space steps are not *a priori* rational).

It is tempting to generalize this idea to nonlinear hyperbolic systems of conservation laws for one-dimensional variables. However, many difficulties occur:

- first, the speed of propagation is not unique and Riemann problems for systems of several equations are expected to generate several waves.
- secondly, due to nonlinear effects, characteristic velocities of the solution vary in space making appear shock or rarefaction waves for genuinely nonlinear characteristic fields.

Clearly, to get $\lambda = 1$ for each characteristic field, and for each computational point, one needs to locally adapt the time step in space, and along each characteristic field. This is precisely the purpose of this paper, which is organized as follows. Section 2 is devoted to the linear hyperbolic system case with constant coefficients. Section 3 deals with nonlinear scalar equations and Section 4 with hyperbolic systems of conservation laws. We will see in this section that any linear or nonlinear approximate Riemann solver as those used in flux schemes may be improved using our methodology. However, for Euler equations and the Colella–Glaz [18] nonlinear Riemann solver, whose principle will be recalled in this paper, numerical results given in Section 5 show a particularly accurate description of both shocks and contact discontinuities as well as nicely computed rarefaction waves.

2. Linear hyperbolic systems

Consider the linear hyperbolic system with m equations:

$$\begin{cases} \partial_t V + \partial_x (AV) = 0, \quad x \in \mathbb{R},\ t \geqslant 0, \\ V(x,0) = V_0(x) \end{cases} \tag{2}$$

with $V = (v_1, \ldots, v_m)^T$, $A \in \mathcal{M}_m(\mathbb{R})$ diagonalizable in $\mathbb{R}$ with eigenvalues $(\lambda_1, \lambda_2, \ldots, \lambda_m)$, and corresponding right eigenvectors $R = \mathrm{col}(r_1, \ldots, r_m)$, associated to the initial data $V_0 \in BV(\mathbb{R})$. Note that the change of variable $W = R^{-1}V = (w_1, \ldots, w_m)^T$, satisfies the following diagonal system of m independent advection equations:

$$\begin{cases} \partial_t w_1 + \lambda_1 \partial_x w_1 = 0, \\ \vdots \\ \partial_t w_m + \lambda_m \partial_x w_m = 0. \end{cases}$$

Let us introduce the flux F defined by $F(V) = AV$. We are looking for an approximation V_j^n of $V(t_n, j\Delta x)$ in (2). The initial data is defined by: $V_j^0 = V_0(j\Delta x)$, $j \in \mathbb{Z}$. Then the classical upwind scheme may be written in this case:

$$V_j^{n+1} = V_j^n - \frac{\Delta t_n}{\Delta x}\big(\Phi_{j+1/2}^n - \Phi_{j-1/2}^n\big), \quad j \in \mathbb{Z},\ n \geqslant 1, \tag{3}$$

where $\Delta t_n = t_{n+1} - t_n$ and $\Phi_{j-1/2}^n$ is the interfacial flux:

$$\Phi_{j-1/2}^n = \frac{F(V_j^n) + F(V_{j-1}^n)}{2} - \frac{1}{2}\operatorname{sgn}(A)\big(F\big(V_j^n\big) - F\big(V_{j-1}^n\big)\big). \tag{4}$$

Here, $\operatorname{sgn}(\cdot)$ is the sign matrix operator given by $\operatorname{sgn}(A) = R\operatorname{diag}_{i=1,\dots,p}(\operatorname{sgn}(\lambda_i))R^{-1}$. We easily see that the scheme can also be written as:

$$W_j^{n+1} = W_j^n - \frac{\Delta t_n}{\Delta x}\, R^{-1}\big(\Phi_{j+1/2}^n - \Phi_{j-1/2}^n\big)$$

with $W_j^n = R^{-1}V_j^n$ or component-wise,

$$\begin{cases} w_{k,j}^{n+1} = w_{k,j}^n - \alpha_k(w_{k,j+1}^n - w_{k,j}^n), & \alpha_k \leqslant 0, \\ w_{k,j}^{n+1} = w_{k,j}^n - \alpha_k(w_{k,j}^n - w_{k,j-1}^n), & \alpha_k > 0, \end{cases}$$

with $\alpha_k = \lambda_k \Delta t_n/\Delta x$, $k = 1, \dots, m$. It is well known that this scheme is ℓ^2-stable under the CFL condition:

$$\alpha \overset{\text{def}}{:=} \frac{\Delta t_n}{\Delta x}\max\big(|\lambda_1|, \dots, |\lambda_m|\big), \quad \text{satisfying } \alpha \leqslant 1. \tag{5}$$

If Δt_n is chosen such that $\alpha = 1$, the propagation is perfectly solved on the components w_k for which $\alpha_k = 1$, and using the analysis done in the introduction, some numerical diffusion will be produced on the other components w_j for which $\alpha_j < 1$. To obtain a CFL equal to one on each characteristic field, let us consider different time steps Δt_n (not necessarily equal). We introduce m vectorial reservoirs $R_{1;j-1/2}, \dots, R_{m;j-1/2} \in \mathbb{R}^m$ associated to the interface $j - 1/2$ and CFL counters $c_{k;j-1/2} \in [0, 1]$, $k = 1, \dots, m$, initialized to zero.

Remark 2.1. Note that for each characteristic field these quantities are constant in space so that spatial indexing is then not necessary. We keep this notation for coherence with forthcoming sections.

We denote by $V_{\mathrm{R}}^k(V, W)$ the solution of the Riemann problem with left state V and right state W which lies between the kth and the $(k+1)$th wave where $V_{\mathrm{R}}^0(V, W) := V$, and $V_{\mathrm{R}}^m(V, W) := W$ by convention. For convenience we introduce a temporary variable:

$$\mathcal{C}_{k;j-1/2}^{n+1} := c_{k;j-1/2}^n + |\lambda_k|\frac{\Delta t_n}{\Delta x}.$$

At each time step we fill up the reservoirs $R_{k;j-1/2}$ with the current numerical flux difference upwinding depending on the sign of λ_k. More precisely, we have for $\lambda_k < 0$, for all n and j

$$\begin{pmatrix} \tilde{V}_{k;j+1/2}^{n+1} \\ c_{k;j+1/2}^{n+1} \\ R_{k;j+1/2}^{n+1} \end{pmatrix} = \begin{cases} \begin{pmatrix} 0 \\ c_{k;j+1/2}^n + |\lambda_k|\dfrac{\Delta t_n}{\Delta x} \\ R_{k;j+1/2}^n - \dfrac{\Delta t_n}{\Delta x}\big(F\big(V_{\mathrm{R}}^k\big(V_j^n, V_{j+1}^n\big)\big) - F\big(V_{\mathrm{R}}^{k-1}\big(V_j^n, V_{j+1}^n\big)\big)\big) \end{pmatrix}, & \text{if } \mathcal{C}_{k;j+1/2}^{n+1} < 1, \\ \begin{pmatrix} R_{k;j+1/2}^n - \dfrac{\Delta t_n}{\Delta x}\big(F\big(V_{\mathrm{R}}^k\big(V_j^n, V_{j+1}^n\big)\big) - F\big(V_{\mathrm{R}}^{k-1}\big(V_j^n, V_{j+1}^n\big)\big)\big) \\ 0 \\ 0 \end{pmatrix}, & \text{if } \mathcal{C}_{k;j+1/2}^{n+1} = 1, \end{cases}$$

whereas, for $\lambda_k > 0$, we upwind on the right side, for all j and n

$$\begin{pmatrix} \tilde{V}^{n+1}_{k;j-1/2} \\ c^{n+1}_{k;j-1/2} \\ R^{n+1}_{k;j-1/2} \end{pmatrix} = \begin{cases} \begin{pmatrix} 0 \\ c^n_{k;j-1/2} + |\lambda_k| \dfrac{\Delta t_n}{\Delta x} \\ R^n_{k;j-1/2} - \dfrac{\Delta t_n}{\Delta x}\big(F\big(V^k_{\mathrm{R}}\big(V^n_{j-1}, V^n_j\big)\big) - F\big(V^{k-1}_{\mathrm{R}}\big(V^n_{j-1}, V^n_j\big)\big)\big) \end{pmatrix}, & \text{if } \mathcal{C}^{n+1}_{k;j-1/2} < 1, \\ \begin{pmatrix} R^n_{k;j-1/2} - \dfrac{\Delta t_n}{\Delta x}\big(F\big(V^k_{\mathrm{R}}\big(V^n_{j-1}, V^n_j\big)\big) - F\big(V^{k-1}_{\mathrm{R}}\big(V^n_{j-1}, V^n_j\big)\big)\big) \\ 0 \\ 0 \end{pmatrix}, & \text{if } \mathcal{C}^{n+1}_{k;j-1/2} = 1. \end{cases} \tag{6}$$

We then update the solution by taking

$$V^{n+1}_j = V^n_j + \sum_{k=1}^{m} \big[\tilde{V}^{n+1}_{k;j-1/2} + \tilde{V}^{n+1}_{k;j+1/2}\big].$$

Above $\tilde{V}$ is simply a temporary variable, introduced to lighten the notations. Note that classical flux schemes are updated by taking (3) with (4). As before, the time step Δt_n must be chosen according to the classical stability condition and as big as possible. This leads to the natural choice

$$\Delta t_n = \min_{j,k} \left((1 - c^n_{k;j-1/2}) \frac{\Delta x}{|\lambda_k|} \right). \tag{7}$$

Example. We show a simple example in order to understand the principle of the reservoir technique. Consider the following diagonal 2×2-system:

$$V_t + \Lambda V_x = 0,$$

with

$$\Lambda = \begin{pmatrix} \lambda_1 & 0 \\ 0 & \lambda_2 \end{pmatrix}.$$

In order to simplify the notations, we also suppose that $2\lambda_1 = \lambda_2 > \lambda_1 > 0$, and the initial data satisfies, for some $j_0 \in \mathbb{Z}$

$$V^0_j = \begin{cases} V^0_{j_0} & \text{if } j \leqslant j_0, \\ V^0_{j_0+1} & \text{if } j > j_0. \end{cases}$$

At the beginning of the process, at each interface $(j + 1/2)\Delta x$ we have to solve a Riemann problem $V_{\mathrm{R}}(V^0_j, V^0_{j+1})$. In our case, the only interface of interest is $(j_0 + 1/2)\Delta x$, we then decompose $V^0_{j_0}$ and $V^0_{j_0+1}$ in the canonical right-eigenbasis $(\mathbf{r}_1, \mathbf{r}_2)$

$$\begin{cases} V^0_{j_0} = \alpha_1 \mathbf{r}_1 + \alpha_2 \mathbf{r}_2, \\ V^0_{j_0+1} = \beta_1 \mathbf{r}_1 + \beta_2 \mathbf{r}_2, \end{cases}$$

and the solution to the Riemann problem at the interface is then given by:

$$V_{\mathrm{R}}(V^0_{j_0}, V^0_{j_0+1}) = \begin{cases} V^0_{j_0} = \alpha_1 \mathbf{r}_1 + \alpha_2 \mathbf{r}_2 & \text{if } x/t < \lambda_1, \\ \beta_1 \mathbf{r}_1 + \alpha_2 \mathbf{r}_2 & \text{if } \lambda_1 < x/t < \lambda_2, \\ V^0_{j_0+1} = \beta_1 \mathbf{r}_1 + \beta_2 \mathbf{r}_2 & \text{if } x/t > \lambda_2. \end{cases}$$

Moreover, since all speeds are nonnegative, all the changes occur in the $(j_0 + 1)$th cell, then we focus our analysis on this cell. In the $(j_0 + 1)$th cell, at time $t_0 = 0$ we initialize reservoirs and counters according to $R^0_{1;j_0+1/2} = R^0_{2;j_0+1/2} = 0$ and $c^0_{1;j_0+1/2} = c^0_{2;j_0+1/2} = 0$. Then:

- The formula (7) leads to $t_1 = t_0 + \Delta t_1$, with $\Delta t_1 = \Delta x/\lambda_2$, and we get $\mathcal{C}^1_{2;\,j_0+1/2} = 1$ then $c^1_{2;\,j_0+1/2} = 0$ and $c^1_{1;\,j_0+1/2} = \lambda_1/\lambda_2 = 1/2$. The update (6) gives

$$\begin{pmatrix} \tilde{V}^1_{2;\,j_0+1/2} \\ c^1_{2;\,j_0+1/2} \\ R^1_{2;\,j_0+1/2} \end{pmatrix} = \left(0 - \frac{\Delta t_1}{\Delta x}\big(F\big(V_{\mathrm{R}}^2\big(V^0_{j_0}, V^0_{j_0+1}\big)\big) - F\big(V_{\mathrm{R}}^1\big(V^0_{j_0}, V^0_{j_0+1}\big)\big)\big), 0, 0\right)^T$$

and

$$\begin{pmatrix} \tilde{V}^1_{1;\,j_0+1/2} \\ c^1_{1;\,j_0+1/2} \\ R^1_{1;\,j_0+1/2} \end{pmatrix} = \left(0, 0 + \lambda_1\frac{\Delta t_1}{\Delta x}, 0 - \frac{\Delta t_1}{\Delta x}\big(F\big(V_{\mathrm{R}}^1\big(V^0_{j_0}, V^0_{j_0+1}\big)\big) - F\big(V_{\mathrm{R}}^0\big(V^0_{j_0}, V^0_{j_0+1}\big)\big)\big)\right)^T$$

$$= \left(0, \frac{1}{2}, -\frac{1}{2}(\beta_1 - \alpha_1)\mathbf{r}_1\right)^T$$

and

$$\begin{aligned} V^1_{j_0+1} &= V^0_{j_0+1} + \tilde{V}^1_{2;\,j_0+1/2} \\ &= V^0_{j_0+1} - \frac{\Delta t_1}{\Delta x}\big(F\big(V_{\mathrm{R}}^2\big(V^0_{j_0}, V^0_{j_0+1}\big)\big) - F\big(V_{\mathrm{R}}^1\big(V^0_{j_0}, V^0_{j_0+1}\big)\big)\big) \\ &= \beta_1\mathbf{r}_1 + \beta_2\mathbf{r}_2 - \frac{\Delta t_1}{\Delta x}\big(F(\beta_1\mathbf{r}_1 + \beta_2\mathbf{r}_2) - F(\beta_1\mathbf{r}_1 + \alpha_2\mathbf{r}_2)\big) \\ &= \beta_1\mathbf{r}_1 + \alpha_2\mathbf{r}_2. \end{aligned}$$

We remark that we catch exactly the intermediate solution to the Riemann problem.

- Afterwards, at time $t_2 = t_1 + \Delta t_2$, and $\Delta t_2 = \Delta t_1$, we get $\mathcal{C}^2_{1;\,j_0+1/2} = 1$ then $c^2_{1;\,j_0+1/2} = 0$ and $c^2_{2;\,j_0+1/2} = \lambda_2/\lambda_1 - 1 = 1$. The reservoirs and the solution are updated according to

$$\begin{pmatrix} \tilde{V}^2_{1;\,j_0+1/2} \\ c^2_{1;\,j_0+1/2} \\ R^2_{1;\,j_0+1/2} \end{pmatrix} = \left(R^1_{1;\,j_0+1/2} - \frac{\Delta t_2}{\Delta x}\big(F\big(V_{\mathrm{R}}^1\big(V^1_{j_0}, V^1_{j_0+1}\big)\big) - F\big(V_{\mathrm{R}}^0\big(V^1_{j_0}, V^1_{j_0+1}\big)\big)\big), 0, 0\right)^T$$

$$= \big((\alpha_1 - \beta_1)\mathbf{r}_1, 0, 0\big)^T$$

and

$$\begin{pmatrix} \tilde{V}^2_{2;\,j_0+1/2} \\ c^2_{2;\,j_0+1/2} \\ R^2_{2;\,j_0+1/2} \end{pmatrix} = \left(0 - \frac{\Delta t_2}{\Delta x}\big(F\big(V_{\mathrm{R}}^2\big(V^1_{j_0}, V^1_{j_0+1}\big)\big) - F\big(V_{\mathrm{R}}^1\big(V^1_{j_0}, V^1_{j_0+1}\big)\big)\big), 0, 0\right)^T$$

$$= (0, 0, 0)^T.$$

This leads to $V^2_{j_0+1} = \alpha_1\mathbf{r}_1 + \alpha_2\mathbf{r}_2$ which is the exact solution at time t_2.

Time steps are chosen such that the waves are exactly located at the mesh interfaces, in the (x, t)-space (see Fig. 3). Such a strategy avoids the creation of numerical diffusion.

3. Nonlinear scalar equation

In this section, we generalize our approach to handle nonlinear effects. We therefore consider a nonlinear scalar conservation law

$$\begin{cases} u_t + f(u)_x = 0, \quad x \in \mathbb{R},\ t \geqslant 0, \\ u(x, 0) = u_0(x) \in BV(\mathbb{R}), \quad x \in \mathbb{R} \end{cases}$$

with f a regular convex function such that $f(0) = 0$. We discretize the solution on a uniform mesh with space step Δx. As usual we search for an approximation u^n_j of the solution $u(t_n, j\Delta x)$.

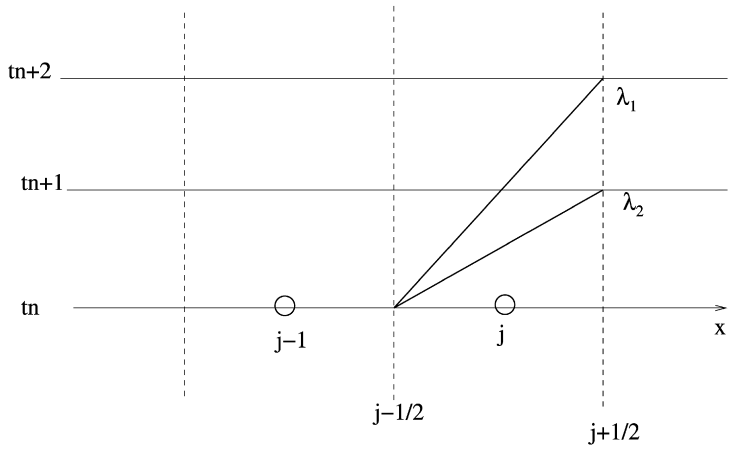

Fig. 3. Intersection of characteristic curves and interfacial vertical lines in the (x,t)-space. A high velocity characteristic field often generates events of updating and reservoir filling.

Remark 3.1. It is well known that nonconvex fluxes lead to much more complex Riemann problems and the extension of the reservoir method in that case, although still doable, is much more complicated and is skipped in this paper.

The initial data is given by: $u_j^0 = u_0(j\Delta x)$, $j \in \mathbb{Z}$. In this case, the classical upwind scheme writes:

$$u_j^{n+1} = u_j^n - \frac{\Delta t_n}{\Delta x}\big(f_{j+1/2}^n - f_{j-1/2}^n\big), \quad j \in \mathbb{Z}, n \geqslant 1,$$

where $f_{j-1/2}^n$ is the interfacial upwinded flux:

$$f_{j-1/2}^n = \frac{f(u_j^n) + f(u_{j-1}^n)}{2} - \frac{1}{2}\operatorname{sgn}(f'(u_{j-1/2}^n))(f(u_j^n) - f(u_{j-1}^n)),$$

with $\Delta t^n = t_{n+1} - t_n$ and $u_{j-1/2}^n$ is an approximate value of the solution at the interface. In the framework of one-dimensional nonlinear scalar equations only two kinds of waves can occur: rarefaction and shock waves. Due to a classical entropy criterion at each interface $j-1/2$ between cells $j-1$ and j, the Lax entropy conditions state that $f'(u_{j-1}^n) > f'(u_j^n)$ for an entropy shock wave while $f'(u_j^n) > f'(u_{j-1}^n)$ generates a rarefaction wave. Let us also recall that from the Rankine–Hugoniot condition, a shock wave at the interface $j-1/2$ has a speed equal to:

$$\sigma_{j-1/2}^n = \frac{f(u_j^n) - f(u_{j-1}^n)}{u_j^n - u_{j-1}^n}.$$

Using this, we propose a method to update reservoirs and counters, upwinding at each interface depending on the sign of $\sigma_{j-1/2}^n$. Let us denote by $\lambda_-^n = f'(u_{j-1}^n)$ and by $\lambda_+^n = f'(u_j^n)$ the left and right characteristic speeds. The idea is to constrain the time step according to the largest wave speed. For shock waves, it is given by Rankine–Hugoniot conditions whereas for rarefaction fans, it is given by the largest speed λ_-^n or λ_+^n. Moreover, in the case of sonic points ($\lambda_-^n \leqslant 0 \leqslant \lambda_+^n$), waves are splitted in two parts, one going to the left and the other one going to the right. We present, the case of waves located at $j-1/2$. Recall here, that we do not consider wave interactions.

– Right shock wave ($0 \leqslant \lambda_+^n \leqslant \lambda_-^n$ and $\sigma_{j-1/2}^n > 0$)

$$\begin{pmatrix} u_j^{n+1} \\ c_{j-1/2}^{n+1} \\ R_{j-1/2}^{n+1} \end{pmatrix} = \begin{cases} \left(u_j^n, c_{j-1/2}^n + \dfrac{|\sigma_{j-1/2}^n|\Delta t_n}{\Delta x}, R_{j-1/2}^n - \dfrac{\Delta t_n}{\Delta x}(f(u_j^n) - f(u_{j-1}^n))\right)^T, \\ \quad \text{if } c_{j-1/2}^n + \dfrac{|\sigma_{j-1/2}^n|\Delta t_n}{\Delta x} < 1, \\ \left(u_j^n + R_{j-1/2}^n - \dfrac{\Delta t_n}{\Delta x}(f(u_j^n) - f(u_{j-1}^n)), 0, 0\right)^T, \quad \text{if } c_{j-1/2}^n + \dfrac{|\sigma_{j-1/2}^n|\Delta t_n}{\Delta x} = 1. \end{cases}$$

– Left shock wave ($\lambda_+^n \leqslant \lambda_-^n \leqslant 0$ and $\sigma_{j-1/2}^n < 0$)

$$\begin{pmatrix} u_{j-1}^{n+1} \\ c_{j-1/2}^{n+1} \\ R_{j-1/2}^{n+1} \end{pmatrix} = \begin{cases} \left(u_{j-1}^n, c_{j-1/2}^n + \dfrac{|\sigma_{j-1/2}^n|\Delta t_n}{\Delta x}, R_{j-1/2}^n - \dfrac{\Delta t_n}{\Delta x}(f(u_j^n) - f(u_{j-1}^n))\right)^T, \\ \quad \text{if } c_{j-1/2}^n + \dfrac{|\sigma_{j-1/2}^n|\Delta t_n}{\Delta x} < 1, \\ \left(u_{j-1}^n + R_{j-1/2}^n - \dfrac{\Delta t_n}{\Delta x}(f(u_j^n) - f(u_{j-1}^n)), 0, 0\right)^T, \quad \text{if } c_{j-1/2}^n + \dfrac{|\sigma_{j-1/2}^n|\Delta t_n}{\Delta x} = 1. \end{cases}$$

– Right rarefaction wave ($\lambda_+^n \geqslant \lambda_-^n \geqslant 0$)

$$\begin{pmatrix} u_{j}^{n+1} \\ c_{j-1/2}^{n+1} \\ R_{j-1/2}^{n+1} \end{pmatrix} = \begin{cases} \left(u_j^n, c_{j-1/2}^n + \dfrac{|\lambda_+^n|\Delta t_n}{\Delta x}, R_{j-1/2}^n - \dfrac{\Delta t_n}{\Delta x}(f(u_j^n) - f(u_{j-1}^n))\right)^T, \quad \text{if } c_{j-1/2}^n + \dfrac{|\lambda_+^n|\Delta t_n}{\Delta x} < 1, \\ \left(u_j^n + R_{j-1/2}^n - \dfrac{\Delta t_n}{\Delta x}(f(u_j^n) - f(u_{j-1}^n)), 0, 0\right)^T, \quad \text{if } c_{j-1/2}^n + \dfrac{|\lambda_+^n|\Delta t_n}{\Delta x} = 1. \end{cases}$$

– Left rarefaction wave ($0 \geqslant \lambda_+^n \geqslant \lambda_-^n$)

$$\begin{pmatrix} u_{j-1}^{n+1} \\ c_{j-1/2}^{n+1} \\ R_{j-1/2}^{n+1} \end{pmatrix} = \begin{cases} \left(u_{j-1}^n, c_{j-1/2}^n + \dfrac{|\lambda_-^n|\Delta t_n}{\Delta x}, R_{j-1/2}^n - \dfrac{\Delta t_n}{\Delta x}(f(u_j^n) - f(u_{j-1}^n))\right)^T, \quad \text{if } c_{j-1/2}^n + \dfrac{|\lambda_-^n|\Delta t_n}{\Delta x} < 1, \\ \left(u_{j-1}^n + R_{j-1/2}^n - \dfrac{\Delta t_n}{\Delta x}(f(u_j^n) - f(u_{j-1}^n)), 0, 0\right)^T, \quad \text{if } c_{j-1/2}^n + \dfrac{|\lambda_-^n|\Delta t_n}{\Delta x} = 1. \end{cases}$$

– Rarefaction wave with sonic point ($\lambda_-^n \leqslant 0 \leqslant \lambda_+^n$). In this very specific situation we have to introduce 2 reservoirs and counters (indices $+$, $-$) at $j - 1/2$, one associated to $j - 1$ and the other one to j such that

$$\begin{pmatrix} u_{j}^{n+1} \\ c_{j-1/2,+}^{n+1} \\ R_{j-1/2,+}^{n+1} \end{pmatrix} = \begin{cases} \left(u_j^n, c_{j-1/2,+}^n + \dfrac{|\lambda_+^n|\Delta t_n}{\Delta x}, R_{j-1/2,+}^n - \dfrac{\Delta t_n}{\Delta x}(f(u_j^n) - f(\bar{u}))\right)^T, \\ \quad \text{if } c_{j-1/2,+}^n + \dfrac{|\lambda_+^n|\Delta t_n}{\Delta x} < 1, \\ \left(u_j^n + R_{j-1/2,+}^n - \dfrac{\Delta t_n}{\Delta x}(f(u_j^n) - f(\bar{u})), 0, 0\right)^T, \quad \text{if } c_{j-1/2,+}^n + \dfrac{|\lambda_+^n|\Delta t_n}{\Delta x} = 1, \end{cases}$$

and then in the cell $j - 1$

$$\begin{pmatrix} u_{j-1}^{n+1} \\ c_{j-1/2,-}^{n+1} \\ R_{j-1/2,-}^{n+1} \end{pmatrix} = \begin{cases} \left(u_{j-1}^n, c_{j-1/2,-}^n + \dfrac{|\lambda_-^n|\Delta t_n}{\Delta x}, R_{j-1/2,-}^n + \dfrac{\Delta t_n}{\Delta x}(f(\bar{u}) - f(u_{j-1}^n))\right)^T, \\ \quad \text{if } c_{j-1/2,-}^n + \dfrac{|\lambda_-^n|\Delta t_n}{\Delta x} < 1, \\ \left(u_{j-1}^n + R_{j-1/2,-}^n + \dfrac{\Delta t_n}{\Delta x}(f(\bar{u}) - f(u_{j-1}^n)), 0, 0\right)^T, \quad \text{if } c_{j-1/2,-}^n + \dfrac{|\lambda_-^n|\Delta t_n}{\Delta x} = 1, \end{cases}$$

where $\bar{u}$ denotes an average state between u_j^n and u_{j-1}^n (a full description of this specific case will be given in a forthcoming paper). A striking effect is that shock-waves and rarefaction waves are handled similarly. The main difference compared to linear equations is that counters are updated differently and some dissipation is introduced in the case of rarefaction waves. Time steps are chosen as usual to be the biggest number ensuring that each counter remains smaller than or equal to 1.

Remark 3.2. In the above analysis, it is important to note that, excepted for sonic points, as we have considered right (resp. left) shock (resp. rarefaction) waves, and as we do not consider wave interactions, waves are always propagated in one single direction (left or right). So that the solution in a cell j is updated with only one single reservoir, $R_{j-1/2}$ for right waves and $R_{j+1/2}$ for left ones.

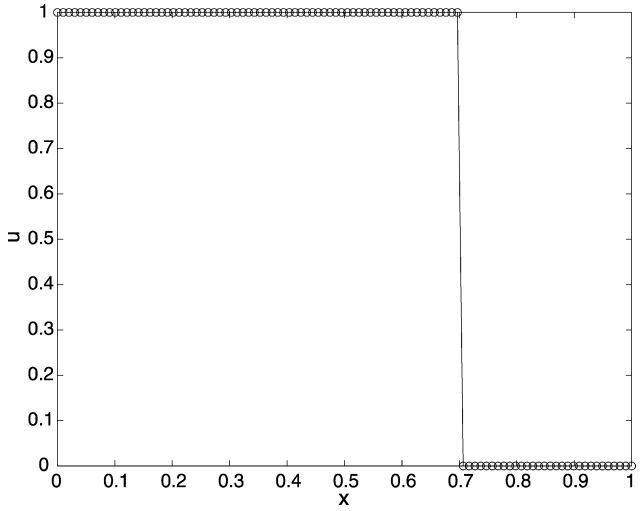

Fig. 4. Reservoir (exact) solution at time $T = 0.4$.

As we can easily observe, the process presented above can become very algorithmically complex. At this stage we do not specify precisely processes allowing to reduce this complexity. However, an optimization of the method is possible based on adapted computations (using lists of time steps and of computed quantities from a cell to another, in particular). This point will be presented in a forthcoming paper.

To illustrate the technique presented above, we propose now a simple numerical example based on the Burger's equation ($f(u) = u^2/2$) and the following initial data.

$$u(x,0) = \begin{cases} 1, & \text{if } x < 1/2, \\ 0, & \text{if } x \geqslant 1/2. \end{cases}$$

The number of grid steps is $N = 100$ and the final time is 0.4. We here update the reservoir solution when CFL counters have reached 0.99. As expected any spurious diffusion is created (see Fig. 4).

4. Nonlinear hyperbolic systems

We now turn to combine the effects of the two previous sections to describe the case of nonlinear hyperbolic systems. Let Ω be an open subset of $\mathbb{R}^m$ and $f : \Omega \to \mathbb{R}^m$ be a sufficiently smooth Lipschitz function. We consider the following nonlinear system of conservation laws:

$$\partial_t V + \partial_x f(V) = 0, \quad x \in \mathbb{R},\ t > 0, \tag{8}$$

where $V = (V_1, \ldots, V_m)^T$ and $f(V) = (f_1(V), \ldots, f_m(V))^T$ and we set

$$A(V) = \left(\frac{\partial f_i}{\partial x_j}(V) \right)_{1 \leqslant i,j \leqslant m}$$

the Jacobian matrix of f. We assume that the system is hyperbolic, that is $A(V)$ is diagonalizable in $\mathbb{R}$. We denote by

$$\lambda_1(V) \leqslant \lambda_2(V) \leqslant \cdots \leqslant \lambda_m(V)$$

the m eigenvalues of $A(V)$ and by $r_k(V)$ (resp. $l_k(V)$) the right (resp. left) eigenvectors of $A(V)$ associated to $\lambda_k(V)$.

4.1. Generalities on reservoirs for nonlinear hyperbolic systems

For such equations we need to define characteristic velocities $\alpha^n_{k;j-1/2}$, at each interface $j - 1/2$ and each characteristic field k. This quantity denotes the velocity of the current wave. Typically, $\alpha^n_{k;j-1/2}$ will be computed using a Riemann solver. We introduce again a temporary variable

$$C^{n+1}_{k;j-1/2} := c^n_{k;j-1/2} + |\alpha^n_{k;j-1/2}| \frac{\Delta t_n}{\Delta x}.$$

Namely, we assume that a Riemann solver (exact or approximate) gives us m waves with related speeds, $\alpha_k(V, W)$ and $m+1$ states $(V_{\mathrm{R}}^k(V, W))_k$ from any left (resp. right) state V (resp. W). More precisely, for $\alpha_{k;j+1/2}^n < 0$ we have

$$\begin{pmatrix} \tilde{V}_{k;j+1/2}^{n+1} \\ c_{k;j+1/2}^{n+1} \\ R_{k;j+1/2}^{n+1} \end{pmatrix} = \begin{cases} \begin{pmatrix} 0 \\ c_{k;j+1/2}^n + |\alpha_{k;j+1/2}^n| \dfrac{\Delta t_n}{\Delta x} \\ R_{k;j+1/2}^n - \dfrac{\Delta t_n}{\Delta x}\big(F\big(V_{\mathrm{R}}^k\big(V_j^n, V_{j+1}^n\big)\big) - F\big(V_{\mathrm{R}}^{k-1}\big(V_j^n, V_{j+1}^n\big)\big)\big) \end{pmatrix}, & \text{if } \mathcal{C}_{k;j+1/2}^{n+1} < 1, \\ \begin{pmatrix} R_{k;j+1/2}^n - \dfrac{\Delta t_n}{\Delta x}\big(F\big(V_{\mathrm{R}}^k\big(V_j^n, V_{j+1}^n\big)\big) - F\big(V_{\mathrm{R}}^{k-1}\big(V_j^n, V_{j+1}^n\big)\big)\big) \\ 0 \\ 0 \end{pmatrix}, & \text{if } \mathcal{C}_{k;j+1/2}^{n+1} = 1, \end{cases} \tag{9}$$

while, for $\alpha_{k;j-1/2}^n > 0$ we set

$$\begin{pmatrix} \tilde{V}_{k;j-1/2}^{n+1} \\ c_{k;j-1/2}^{n+1} \\ R_{k;j-1/2}^{n+1} \end{pmatrix} = \begin{cases} \begin{pmatrix} 0 \\ c_{k;j-1/2}^n + |\alpha_{k;j-1/2}^n| \dfrac{\Delta t_n}{\Delta x} \\ R_{k;j-1/2}^n - \dfrac{\Delta t_n}{\Delta x}\big(F\big(V_{\mathrm{R}}^k\big(V_{j-1}^n, V_j^n\big)\big) - F\big(V_{\mathrm{R}}^{k-1}\big(V_{j-1}^n, V_j^n\big)\big)\big) \end{pmatrix}, & \text{if } \mathcal{C}_{k;j-1/2}^{n+1} < 1, \\ \begin{pmatrix} R_{k;j-1/2}^n - \dfrac{\Delta t_n}{\Delta x}\big(F\big(V_{\mathrm{R}}^k\big(V_{j-1}^n, V_j^n\big)\big) - F\big(V_{\mathrm{R}}^{k-1}\big(V_{j-1}^n, V_j^n\big)\big)\big) \\ 0 \\ 0 \end{pmatrix}, & \text{if } \mathcal{C}_{k;j-1/2}^{n+1} = 1. \end{cases} \tag{10}$$

The reservoir method simply consists in computing the values $\alpha_{l;j-1/2}^n$ according to the corresponding wave speed given by the Riemann solver and the corresponding eigenvalue of the Jacobian matrix of the physical flux on left and right states. This is done in the spirit of Section 3 for each wave separately. Namely, denoting by $\lambda_{l;j}^n = \lambda_l(V_j^n)$, we define $\alpha_{l;j-1/2}^n$ by

$$\forall l \in \{1, \dots, m\},\ \forall j \in \mathbb{Z} \quad \begin{cases} \alpha_{l;j-1/2}^n = \lambda_{l;j-1}^n \quad \text{if } 0 \leqslant \lambda_{l;j-1}^n \leqslant \lambda_{l;j}^n, \text{ for right-rarefaction waves,} \\ \alpha_{l;j-1/2}^n = \lambda_{l;j}^n \quad \text{if } \lambda_{l;j-1}^n \leqslant \lambda_{l;j}^n \leqslant 0, \text{ for left-rarefaction waves,} \\ \alpha_{l;j-1/2}^n = \sigma_{l;j-1/2}^n, \quad \text{for shock waves } (\lambda_{l;j-1}^n > \sigma_{l;j-1/2}^n > \lambda_{l;j}^n), \\ \text{For sonic points, see Remark 4.2.} \end{cases} \tag{11}$$

Again, the solution is updated the following manner

$$V_j^{n+1} = V_j^n + \sum_{k=1}^{m} \big[\tilde{V}_{k;j+1/2}^{n+1} + \tilde{V}_{k;j-1/2}^{n+1}\big],$$

with $\tilde{V}$ the intermediate sequence defined above.

Remark 4.1. Note that for $m = 1$, the reservoir scheme degenerates into the scheme presented in Section 3.

Remark 4.2. In the case of a rarefaction wave with sonic points, that is $\lambda_{l;j-1}^n \leqslant 0 \leqslant \lambda_{l;j}^n$ for a particular $l \in \{1, \dots, m\}$, we follow the procedure detailed in Section 3.

4.2. Application of the reservoir technique to flux schemes

A reservoir technique is presented for a general class of finite volume schemes called flux schemes [19].

Remark 4.3. Roe scheme [20], VFFC (Volumes Finis à Flux Caractéristiques) scheme [21] are flux schemes based on approximate Riemann solvers.

Flux schemes [22] approximate equation (8) by:

$$V_j^{n+1} = V_j^n - \frac{\Delta t}{\Delta x}\big(g\big(V_j^n, V_{j+1}^n\big) - g\big(V_{j-1}^n, V_j^n\big)\big)$$

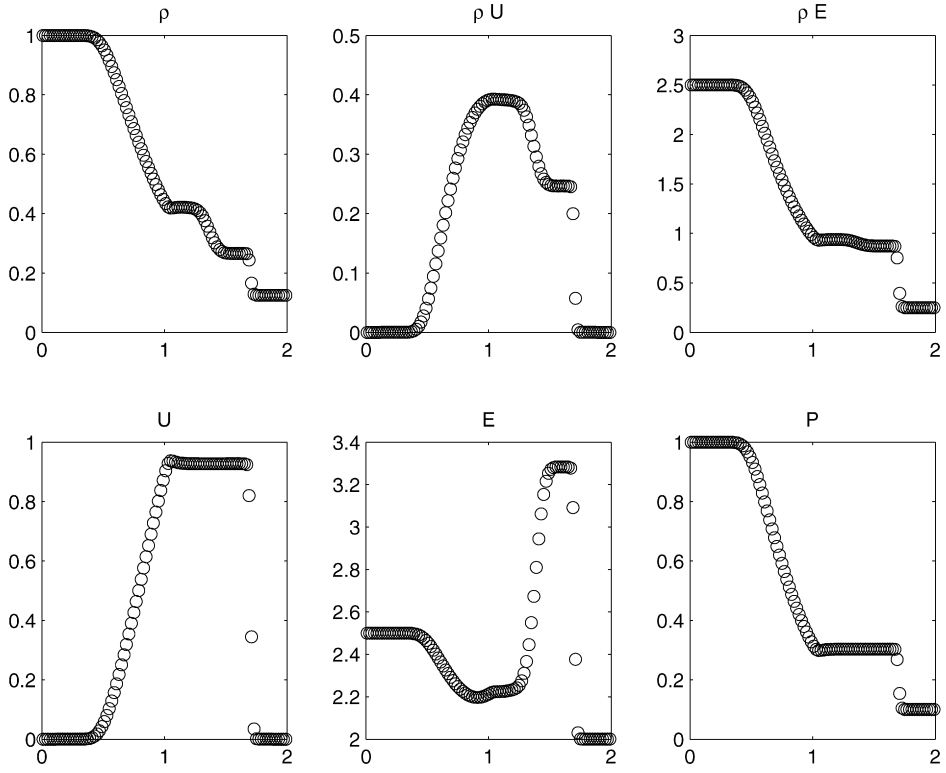

Fig. 5. Results at $t = 0.4$ s of VFFC scheme on Sod tube.

where the numerical flux g is usually given by

$$g(u,v) = \frac{1}{2}\big(f(u) + f(v)\big) - \frac{1}{2}\Lambda(u,v)\big(f(v) - f(u)\big),$$

and Λ is a sign matrix (see [21] or [19]). The reservoir version of flux schemes is straightforward. Consider the cell j at time $t = t_n$ such that $R^n_{l;j-1/2} = 0$ and $c^n_{l;j-1/2} = 0$.

The specificity is that we use at each interface a linearized Riemann solver. For the sake of simplicity we suppose that the system is strictly hyperbolic:

$$\lambda_1(u) < \lambda_2(u) < \cdots < \lambda_m(u).$$

At each interface $(j - 1/2)\Delta x$, we decompose the flux difference $f(V^n_j) - f(V^n_{j-1})$ in the right-eigenbasis of the Jacobian matrix associated to the interfacial state $V_{j-1/2}$ (for instance the average between V^n_j and V^n_{j-1}). That is:

$$f\big(V^n_j\big) - f\big(V^n_{j-1}\big) = \sum_{k=1}^{m} \lambda^n_{k;j-1/2}\gamma^n_{k;j-1/2}\mathbf{r}^n_{k;j-1/2}.$$

The flux scheme consists in considering the propagation speeds as $\lambda^n_{k;j-1/2}$, and the flux difference between neighboring states of the Riemann problem is approximated by:

$$f\big(V^{k+1}_{\mathrm{R}}\big(V^n_{j-1}, V^n_j\big)\big) - f\big(V^k_{\mathrm{R}}\big(V^n_{j-1}, V^n_j\big)\big) = \lambda^n_{k;j-1/2}\gamma^n_{k;j-1/2}\mathbf{r}^n_{k;j-1/2}, \quad \forall k \in \{1,\ldots,m\}. \tag{12}$$

The reservoir version of flux schemes and consists for shock waves of taking $\alpha^n_{l;j-1/2} = \lambda^n_{l;j-1/2}$ in (11) and the aforementioned approximation (12) in (9), (10). In Figs. 5 and 6, we show the results obtained with VFFC at CFL close to one and with VFFC coupled with the reservoir technique. The benchmark we consider here is the Sod tube. Results show a slight improvement (see the rarefaction wave) but nothing spectacular. This is due to the linearized Riemann solver giving a nonaccurate enough wave decomposition. In the sequel we implement the Colella–Glaz Riemann solver [18] in order to remedy to that point.

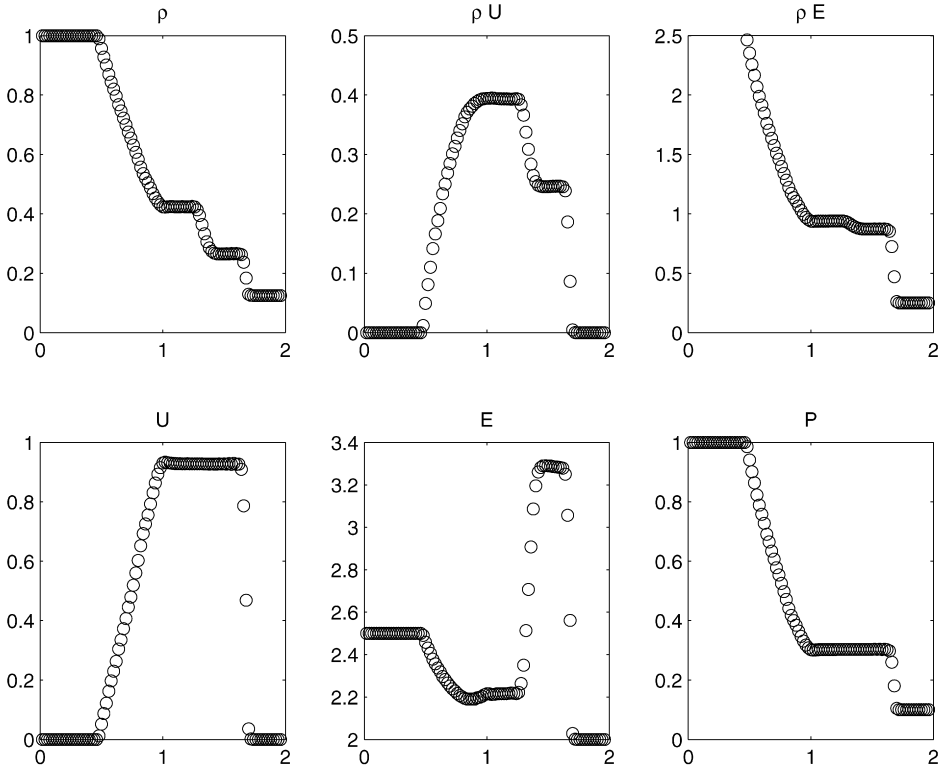

Fig. 6. Results at $t = 0.4$ s on Sod tube with VFFC plus reservoirs.

4.3. Colella–Glaz solver for gas dynamics

The aim of this section is to give a general description of the Colella–Glaz scheme for hyperbolic system of conservation laws (8).

The main idea in [18] is to enforce solutions of a Riemann problem to be a succession of shock waves (or contact discontinuities). Since shock curves (in particular for nonentropic shocks) are close to rarefaction curves, this procedure turns out to be very precise to find accurate intermediate states, with a cost much less than a full nonlinear entropic Riemann solver [23].

Remark 4.4. The approximate Riemann solver involved in this method is also known as the shock curve intersection method. Mehlman [24] has reinterpreted the Colella–Glaz scheme as a particular Roe scheme.

The flux difference is decomposed as:

$$f\big(V_j^n\big) - f\big(V_{j+1}^n\big) = \sum_{k=1}^{m} \big(f\big(V_{\mathrm{R}}^{k-1}\big(V_j^n, V_{j+1}^n\big)\big) - f\big(V_{\mathrm{R}}^{k}\big(V_j^n, V_{j+1}^n\big)\big)\big). \tag{13}$$

Since all the waves are shock waves then (13) can be rewritten as

$$f\big(V_j^n\big) - f\big(V_{j+1}^n\big) = \sum_{k=1}^{k=m} s_{k;\,j+1/2}^n \big(V_{\mathrm{R}}^{k-1}\big(V_j^n, V_{j+1}^n\big) - V_{\mathrm{R}}^{k}\big(V_j^n, V_{j+1}^n\big)\big). \tag{14}$$

In (14) $s_{1;\,j+1/2}^n < \cdots < s_{m;\,j+1/2}^n$ are defined as shock velocities given by the Rankine–Hugoniot equations. Let us again denote by $V_{\mathrm{R}}^k(V_j^n, V_{j+1}^n)$ the kth state, with, by convention, $V_{\mathrm{R}}^0(V_j^n, V_{j+1}^n) = V_j^n$. Since all the states $V_{\mathrm{R}}^k(V_j^n, V_{j+1}^n)$ and speeds $s_{k;\,j+1/2}^n$ are $(2m-1)$ unknowns, the problem turns out to solve the nonlinear Rankine–Hugoniot equations ($2m-1$ equations):

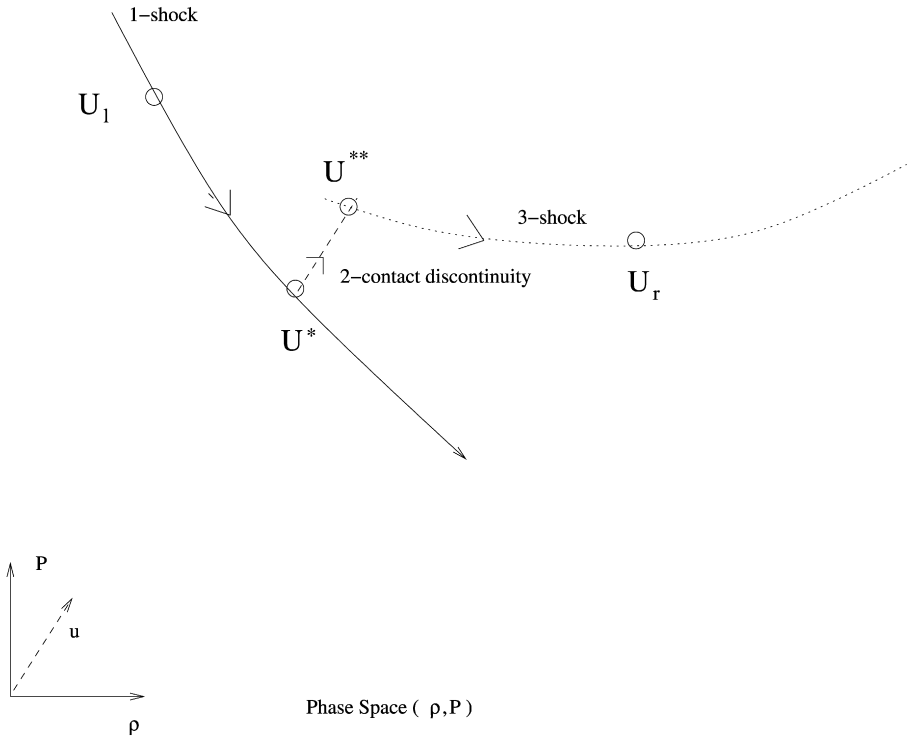

Fig. 7. Colella–Glaz solver.

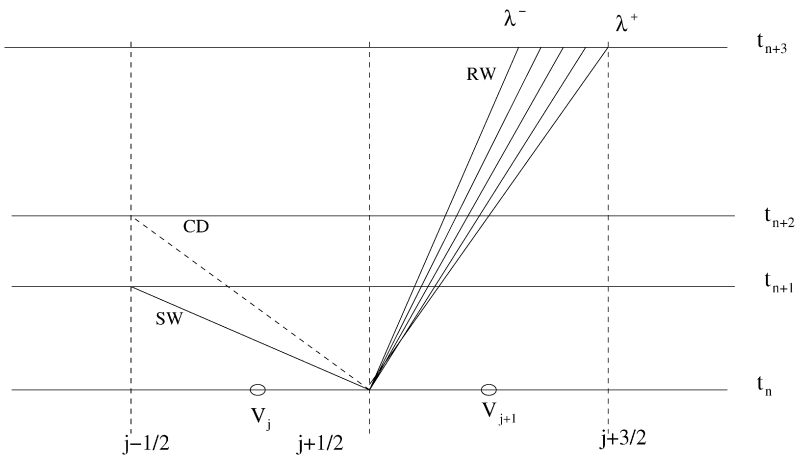

Fig. 8. Time step choice.

$$s^n_{k;j+1/2}\big(V^k_{\mathrm{R}}(V^n_j, V^n_{j+1}) - V^{k-1}_{\mathrm{R}}(V^n_j, V^n_{j+1})\big) = f\big(V^k_{\mathrm{R}}(V^n_j, V^n_{j+1})\big) - f\big(V^{k-1}_{\mathrm{R}}(V^n_j, V^n_{j+1})\big).$$

In [18] a numerical process is given to solve this system for Euler equations and weak shocks (see Figs. 7, 8).

Remark 4.5. For classical compressible Euler equations the second wave is a contact discontinuity, so that the non-linear system can be simplified.

At this point we can now extend the reservoir technique to the Colella–Glaz scheme by taking $\sigma^n_{l;j-1/2} = s^n_{l;j-1/2}$ in (11) and the aforementioned approximation (12) in (9), (10). This is summarized in Fig. 8.

Table 1
Initial data

Benchmark	ρ_l	u_l	p_l	ρ_r	u_r	p_r	$T_{\max}$	γ	N
Sod tube	1	0.75	1	0.125	0	0.1	0.4	1.4	100
Noh	1	1	10^{-6}	1	-1	10^{-6}	0.4	5/3	100
Montagne, Vinokur, Yee	0.01	2200	573	0.14	0	22300	0.2	1.4	100
Wendroff benchmark	1	1	1e − 6	2	-1	1e − 6	1	5/3	100
3a benchmark	1	−19.59745	1000	1	−19.59745	0.01	0.012	1.4	100
Sod Wendroff tube	1	0.75	1	0.125	0	0.1	0.2	1.4	100

5. Numerical results

We now present some numerical experiments to validate the reservoir technique coupled with the Colella–Glaz solver. We consider Euler equations, since it represents a classical nonlinear hyperbolic system of conservation laws with a large literature and many referenced benchmarks.

$$\begin{cases} \rho_t + (\rho u)_x = 0, \\ (\rho u)_t + (\rho u^2 + P)_x = 0, \\ (\rho E)_t + (\rho u H)_x = 0, \quad E = \dfrac{1}{2}u^2 + \dfrac{1}{\gamma - 1}\dfrac{p}{\rho}, \quad H = E + \dfrac{p}{\rho}, \quad \gamma = 1.4. \end{cases}$$

One-dimensional shock tube problems allow to obtain any kind of wave (rarefaction, shock waves and contact discontinuities). We here decide to reproduce some benchmarks presented in [25] that constitutes a very good framework to test one-dimensional hyperbolic solvers. Initial data are given in Table 1. It is important to note that for particular benchmarks a "CFL = 1" method is necessary to obtain correct solutions. For example Berthon in [26] shows that the numerical diffusion created by classical schemes can lead to totally unphysical solutions and forbids the convergence of the scheme. In the following we present the results obtained with the reservoir technique with 2 visualization strategies. The first one is obtained by emptying the reservoirs at final time so that some mixing (and thus some moderated numerical diffusion) appears through shock waves (see Figs. 9, 11, 13, 15, 17, 19) with discrete shock profiles spread over one point at worst. We emphasize that the discrete solutions are conservative and totally consistent with the continuous problem. In the second visualization strategy we present the results without emptying the residual reservoirs at final time, that is without numerical diffusion in the shock waves (Figs. 10, 12, 14, 16, 18, 20). The only difference with the previous visualization comes from the fact that the displayed numerical solution is not fully consistent with the continuous solution. The results obtained here are often far better from than those obtained by other standard numerical methods (see [25] for a systematic comparison) even in theses simulations we have emptied the reservoirs when local counters have reached 0.99 (and not 1). This then allowed to create very few diffusion necessary to remain stable in time. For example the results obtained using the reservoir technique for the Noh test case are particularly better than those obtained by usual high order schemes, like ENO or WENO schemes [27]. In general rarefaction as well as shock waves are very accurately approximated (see [28]). In particular the "zero-point shock capturing" feature is a outstanding behavior for a first order difference scheme. To our knowledge, only the Glimm scheme has a similar behavior, unfortunately Glimm scheme does not capture shocks at the correct position because of its intrinsic random process.

6. Conclusion

We have presented a new low/zero diffusive numerical technique for first order accurate finite volume schemes by enforcing a local field-by-field "CFL one"-like condition on each cell and each characteristic field. The method is based on the use of some cell-by-cell reservoirs and CFL counters that reduce the mixing of information or, in other words, the production of spurious numerical diffusion. This general technique is particularly suited for the Colella–Glaz solver and gives impressive results compared to other classical finite volume schemes even if high order reconstructions (ENO, WENO) are used (see [27]). We also would like to emphasize the fact that the reservoir approach can be more generally applied to any Godunov-type scheme or any flux scheme like VFFC [19]. In this case, results are not that outstanding, but improve the resolution of rarefaction fans without high order reconstruction.

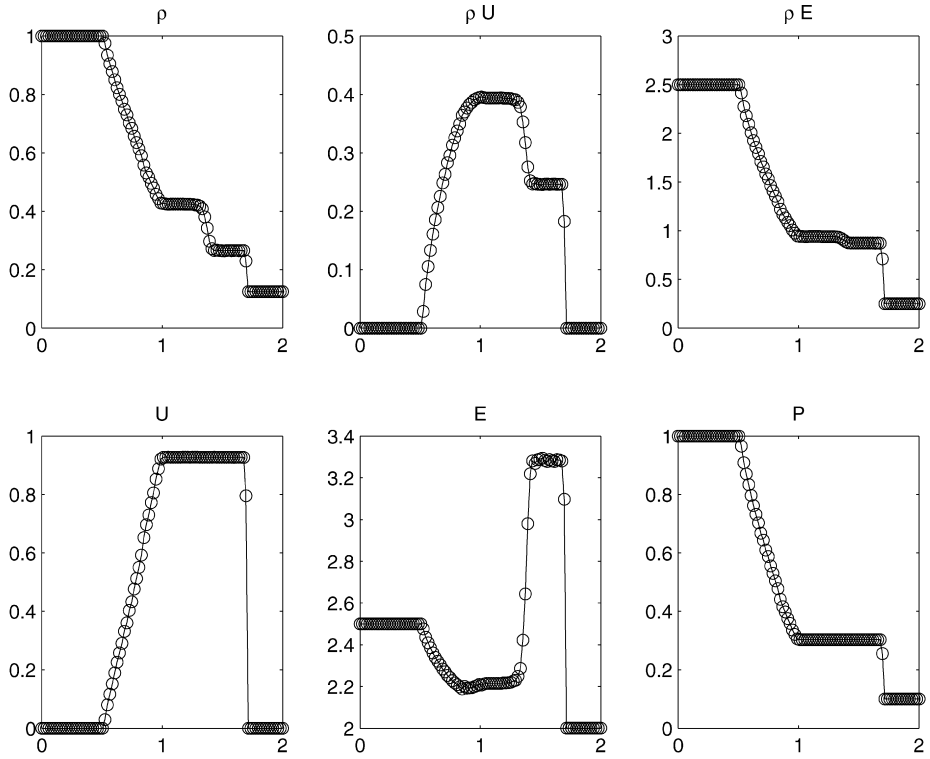

Fig. 9. Sod tube with Colella–Glaz reservoir when residual reservoirs are emptied at final time (first visualization strategy).

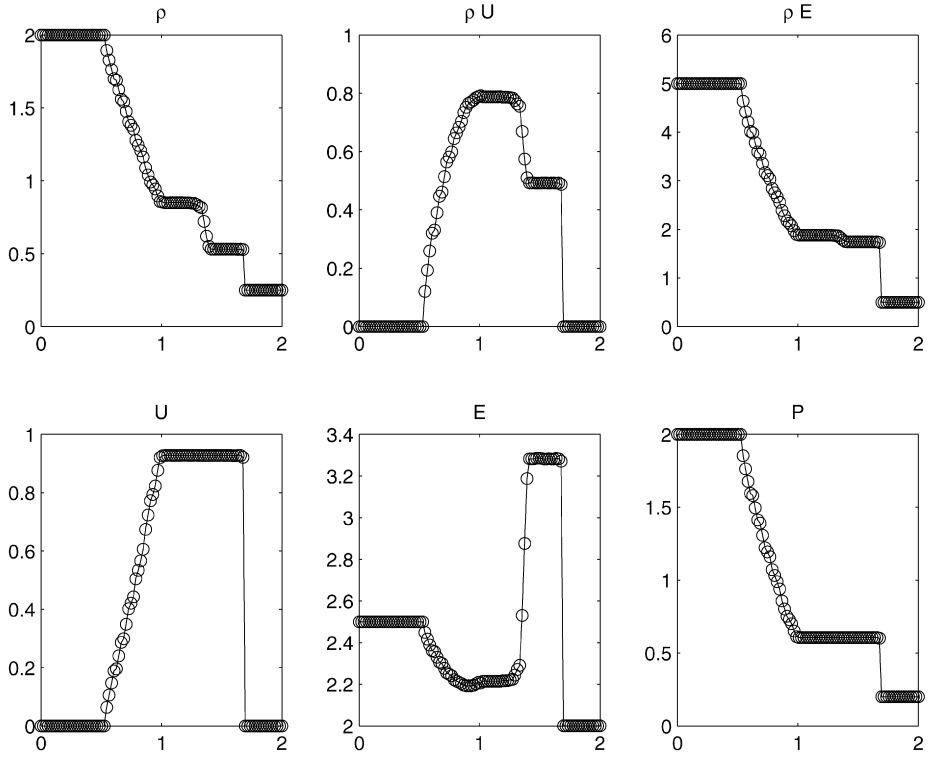

Fig. 10. Sod tube with Colella–Glaz reservoir when residual reservoirs are not emptied at final time (second visualization strategy).

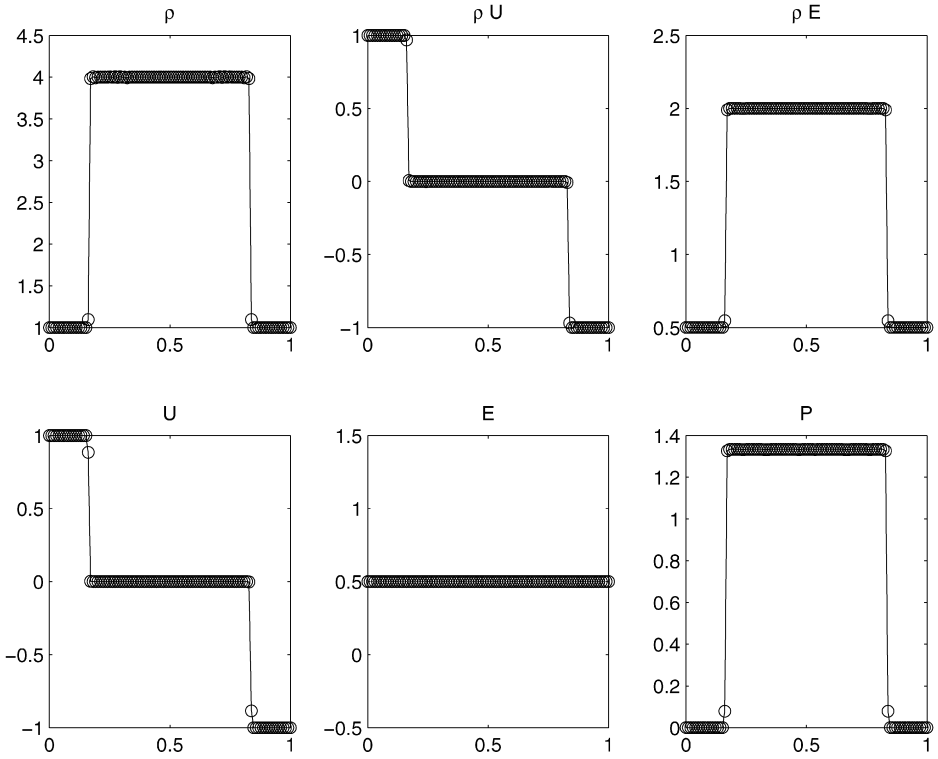

Fig. 11. Noh benchmark with Colella–Glaz reservoir when residual reservoirs are emptied at final time.

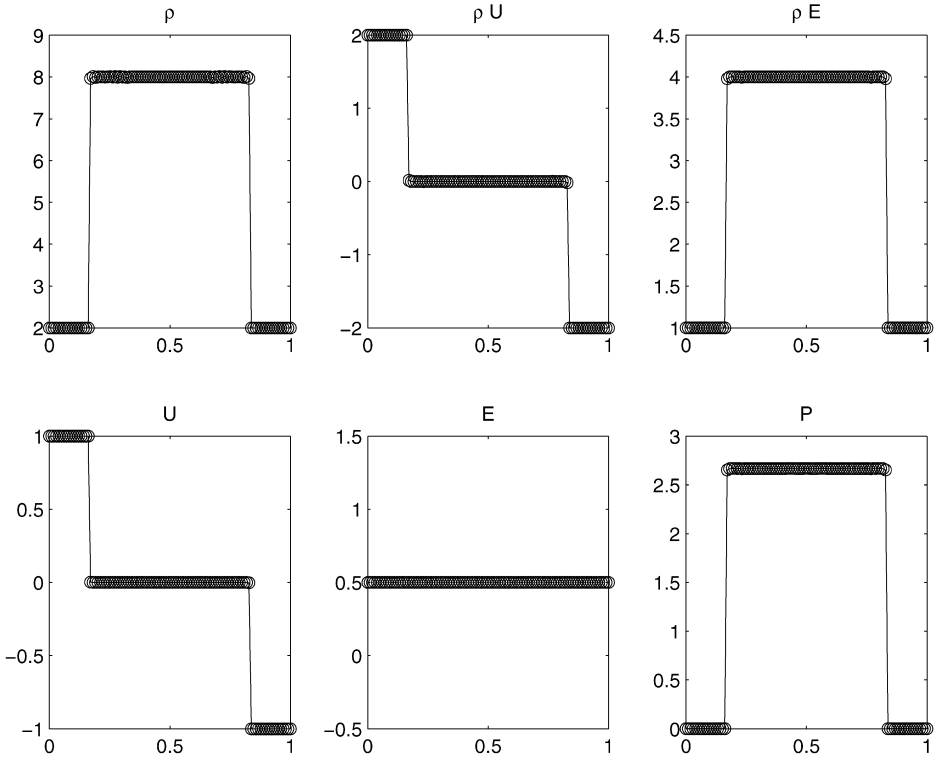

Fig. 12. Noh benchmark with Colella–Glaz reservoir when residual reservoirs are not emptied at final time.

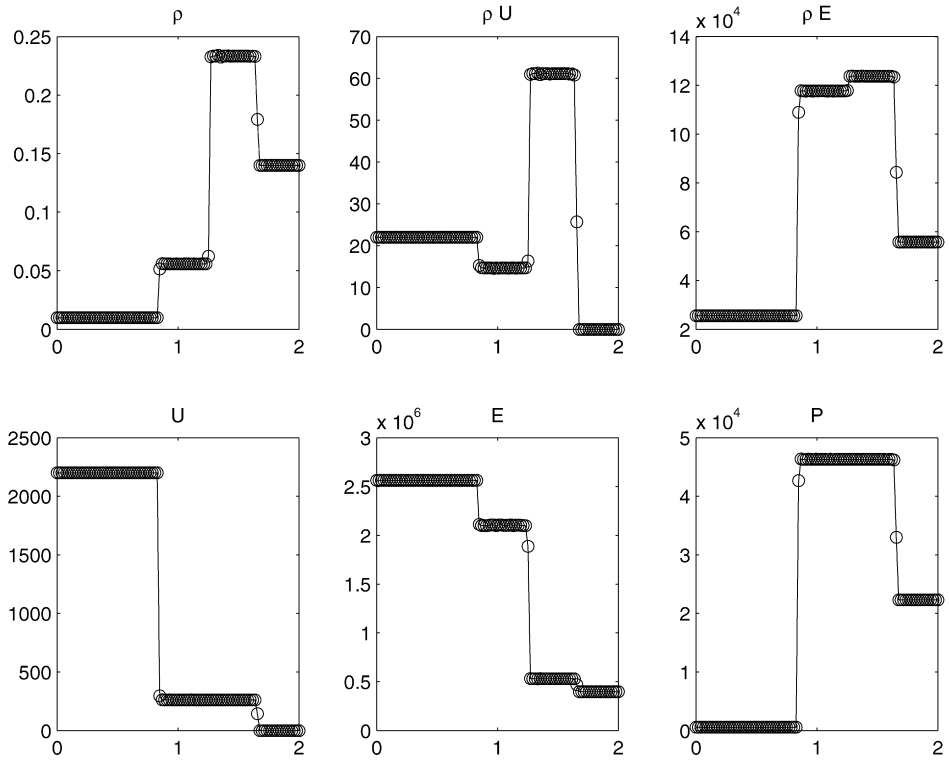

Fig. 13. Montagne, Vinokur, Yee benchmark with Colella–Glaz reservoir when residual reservoirs are emptied at final time.

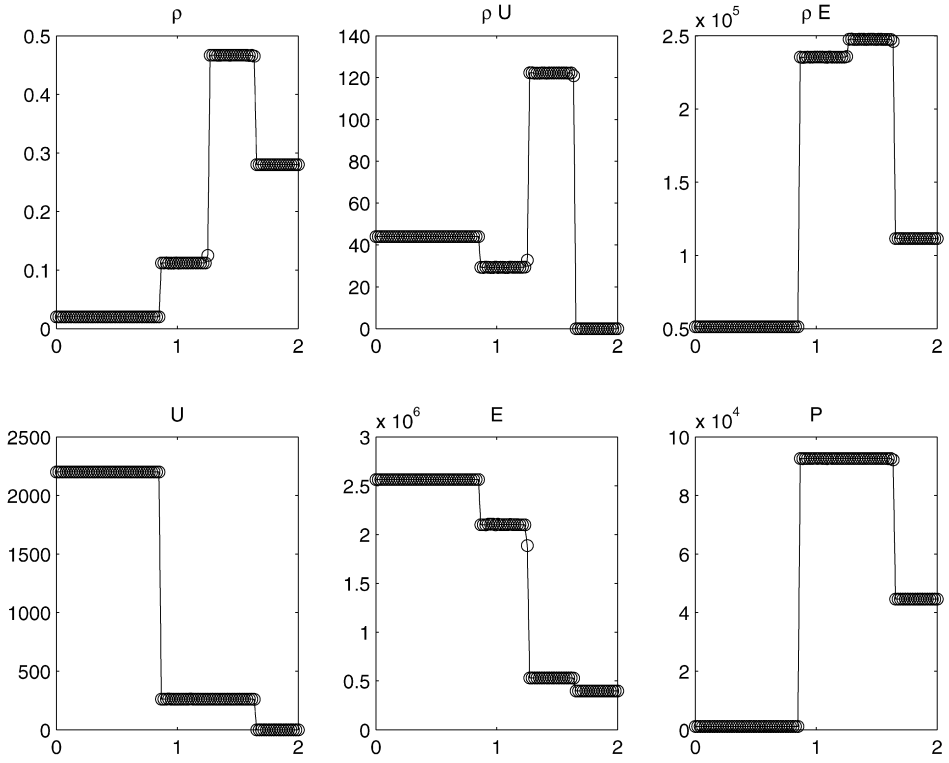

Fig. 14. Montagne, Vinokur, Yee benchmark with Colella–Glaz reservoir when residual reservoirs are not emptied at final time.

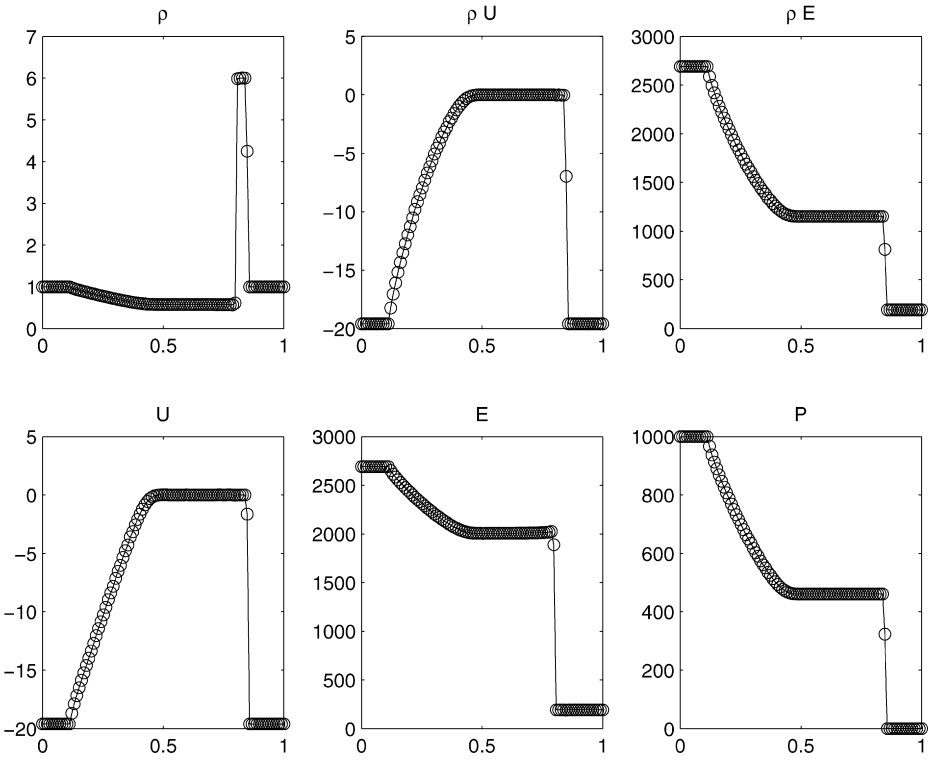

Fig. 15. (3a) benchmark with Colella–Glaz reservoir when residual reservoirs are emptied at final time.

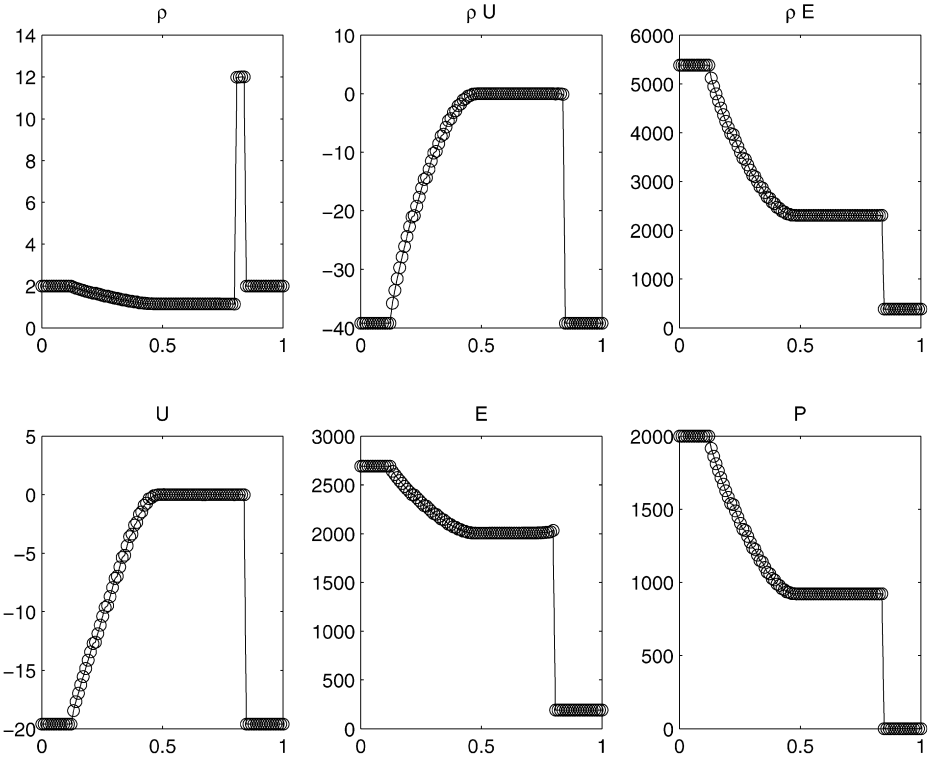

Fig. 16. (3a) benchmark with Colella–Glaz reservoir when residual reservoirs are not emptied at final time.

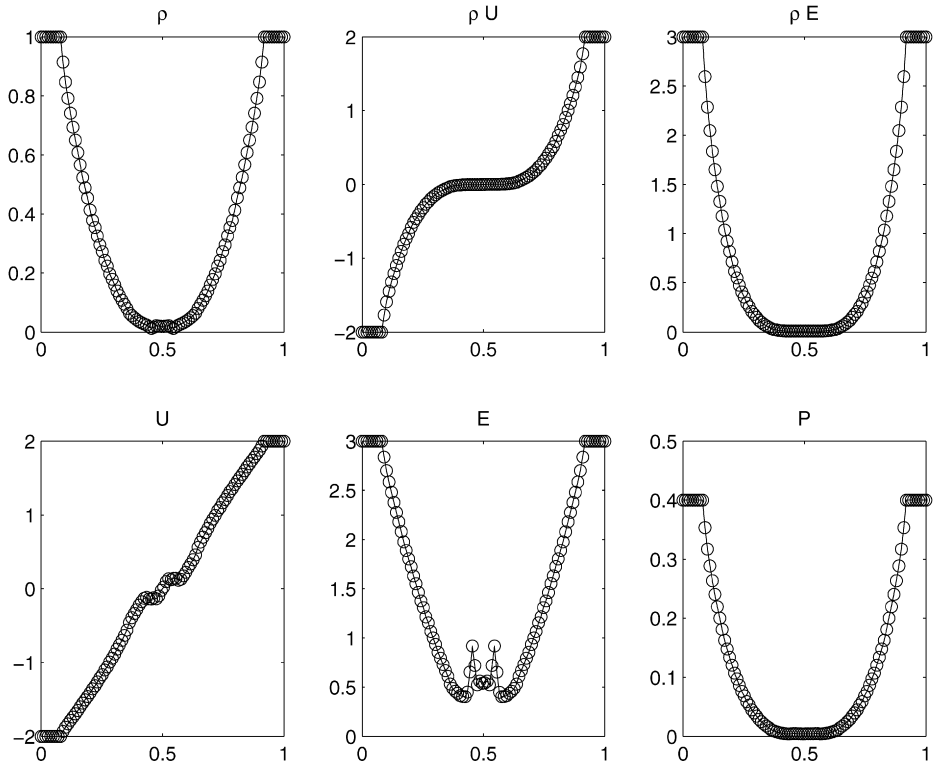

Fig. 17. Wendroff benchmark with Colella–Glaz reservoir when residual reservoirs are emptied at final time.

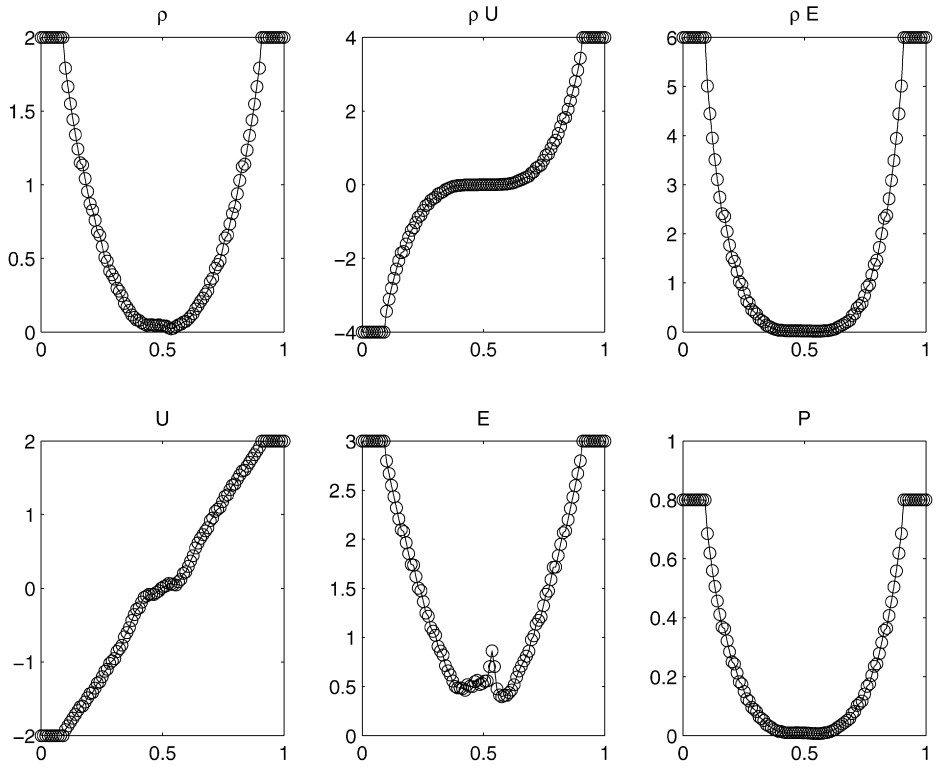

Fig. 18. Wendroff benchmark with Colella–Glaz reservoir when residual reservoirs are not emptied at final time.

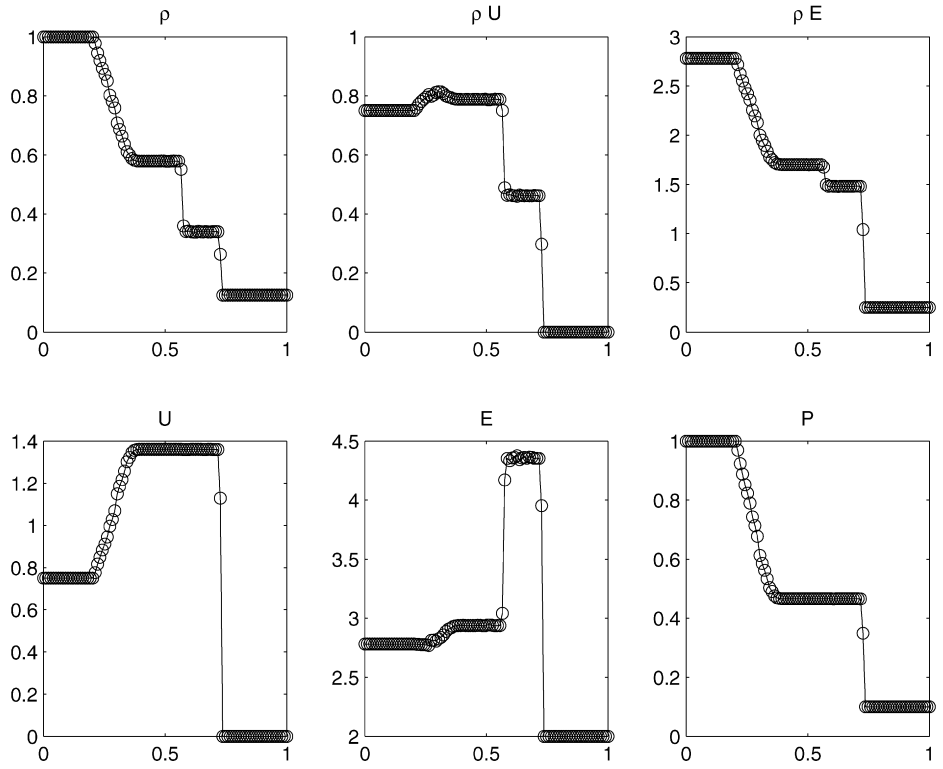

Fig. 19. Sod Wendroff tube with Colella–Glaz reservoir when residual reservoirs are emptied at final time.

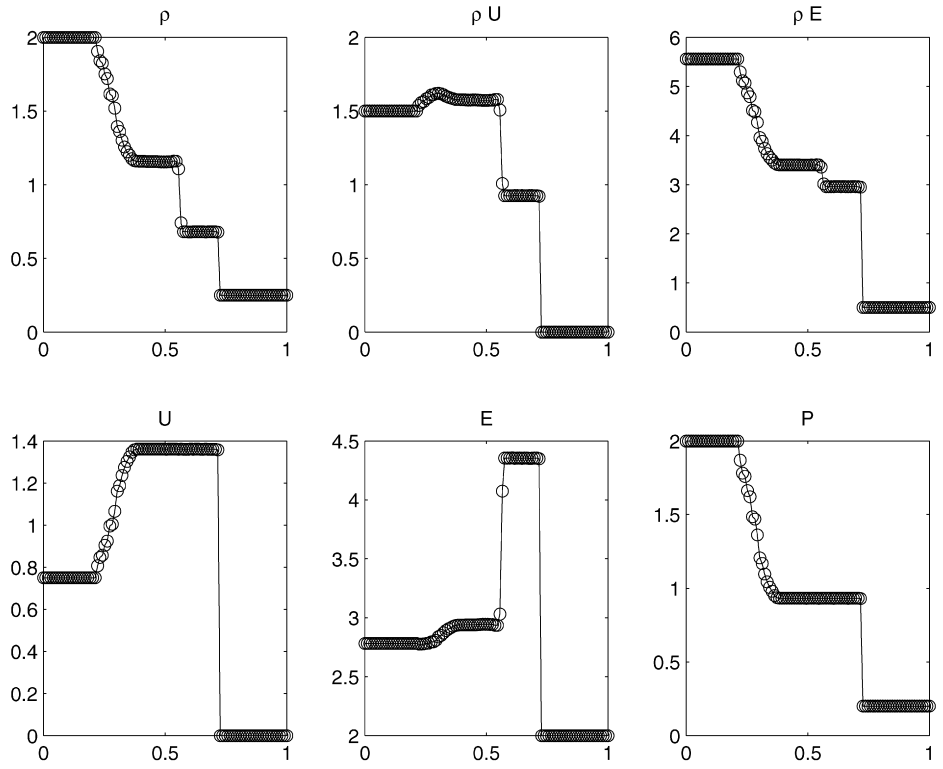

Fig. 20. Sod Wendroff tube with Colella–Glaz reservoir when residual reservoirs are not emptied at final time.

Practically, the reservoir approach can be seen as a finer integration process and can easily be integrated into an existing computational code based on Godunov-type method.

The convergence of this method is presented in [28] and its extension to multidimensional equations is proposed in [29].

At the current time it is still necessary to optimize the technique in term of algorithmic complexity and also to extend it to implicit finite volume schemes. We also think that the Colella–Glaz solver could be extended to more general systems than Euler equations, like two-phase or two-fluid systems (see the paper of Alouges and Merlet [30]).

References

[1] F. Alouges, F. De Vuyst, G. Le Coq, E. Lorin, Un procédé de réduction de la diffusion numérique des schémas à différence de flux d'ordre un pour les systèmes hyperboliques non linéaires, C. R. Math. Acad. Sci. Paris, Ser. I 335 (7) (2002) 627–632.
[2] F. Alouges, F. De Vuyst, G. Le Coq, E. Lorin, The reservoir scheme for systems of conservation laws, in: Finite Volumes for Complex Applications, III, Porquerolles, 2002, Lab. Anal. Topol. Probab. CNRS, Marseille, 2002, pp. 247–254 (electronic).
[3] B.-Y. Guo, H.-P. Ma, E. Tadmor, Spectral vanishing viscosity method for nonlinear conservation laws, SIAM J. Numer. Anal. 39 (4) (2001) 1254–1268 (electronic).
[4] A. Cohen, S.M. Kaber, S. Müller, M. Postel, Fully adaptive multiresolution finite volume schemes for conservation laws, Math. Comp. 72 (241) (2003) 183–225 (electronic).
[5] G.-S. Jiang, C.-W. Shu, Efficient implementation of weighted ENO schemes, J. Comput. Phys. 126 (1) (1996) 202–228.
[6] C.-W. Shu, S. Osher, Efficient implementation of essentially nonoscillatory shock-capturing schemes, J. Comput. Phys. 77 (2) (1988) 439–471.
[7] A. Harten, High resolution schemes for hyperbolic conservation laws, J. Comput. Phys. 49 (3) (1983) 357–393.
[8] P.K. Sweby, High resolution schemes using flux limiters for hyperbolic conservation laws, SIAM J. Numer. Anal. 21 (5) (1984) 995–1011.
[9] F. Bouchut, B. Christian, P. Benoit, A muscl method satisfying all the numerical entropy inequalities, Math. Comp. 65 (1996) 1339–1461.
[10] B. Després, F. Lagoutière, Contact discontinuity capturing schemes for linear advection and compressible gas dynamics, J. Sci. Comput. 16 (4) (2001) 479–524.
[11] F. Coquel, P.G. LeFloch, An entropy satisfying MUSCL scheme for systems of conservation laws, Numer. Math. 74 (1) (1996) 1–33.
[12] F. Coquel, P.G. LeFloch, Un schéma entropique du second ordre pour les systèmes de lois de conservation, C. R. Acad. Sci. Paris, Sér. I Math. 320 (10) (1995) 1263–1268.
[13] B. Després, F. Lagoutière, Un schéma non linéaire anti-dissipatif pour l'équation d'advection linéaire, C. R. Acad. Sci. Paris Sér. I Math. 328 (10) (1999) 939–944.
[14] F. Bouchut, An antidiffusive entropy scheme for monotone scalar conservation laws, J. Sci. Comput. 21 (1) (2004) 1–30.
[15] Z. Xu, C.-W. Shu, Anti-diffusive flux corrections for high order finite difference WENO schemes, J. Comput. Phys. 205 (2) (2005) 458–485.
[16] S. Clerc, Accurate computation of contact discontinuity in flows with general equations of state, Comput. Methods Appl. Mech. Engrg. 178 (1999) 245–255.
[17] T.Y. Hou, P.G. LeFloch, Why nonconservative schemes converge to wrong solutions: error analysis, Math. Comp. 62 (206) (1994) 497–530.
[18] P. Colella, H.M. Glaz, Efficient solution algorithms for the Riemann problem for real gases, J. Comput. Phys. 59 (2) (1985) 264–289.
[19] J.-M. Ghidaglia, A. Kumbaro, G. Le Coq, M. Tajchman, A finite volume implicit method based on characteristic flux for solving hyperbolic systems of conservation laws, in: Proceedings of the Conference on Nonlinear Evolution Equations and Infinite-dimensional Dynamical Systems, Shanghai, 1995, World Sci. Publishing, River Edge, NJ, 1997, pp. 50–65.
[20] P.L. Roe, Approximate Riemann solvers, parameter vectors, and difference schemes, J. Comput. Phys. 43 (2) (1981) 357–372.
[21] J.-M. Ghidaglia, A. Kumbaro, G. Le Coq, Une méthode "volumes finis" à flux caractéristiques pour la résolution numérique des systèmes hyperboliques de lois de conservation, C. R. Acad. Sci. Paris Sér. I Math. 322 (10) (1996) 981–988.
[22] J.-M. Ghidaglia, G. Le Coq, I. Toumi, Two flux-schemes for computing two-phases flows through multi-dimensional finite element methods, Technical report, Prépublication du CMLA, 1999.
[23] J. Smoller, Shock Waves and Reaction–Diffusion Equations, Grundlehren der Mathematischen Wissenschaften (Fundamental Principles of Mathematical Science), vol. 258, Springer-Verlag, New York, 1983.
[24] G. Mehlman, An approximate Riemann solver for fluid systems based on a shock curve decomposition, in: Third International Conference on Hyperbolic Problems, vols. I, II, Uppsala, 1990, Studentlitteratur, Lund, 1991, pp. 727–741.
[25] R. Liska, B. Wendroff, Comparison of several difference schemes on 1D and 2D test problems for the Euler equations, SIAM J. Sci. Comput. 25 (3) (2003) 995–1017 (electronic).
[26] C. Berthon, B. Nkonga, Behavior of the finite volumes schemes in material and numerical interfaces, in: Finite Volumes for Complex Applications, III, Porquerolles, 2002, Lab. Anal. Topol. Probab. CNRS, Marseille, 2002, pp. 125–132 (electronic).
[27] C.-W. Shu, High order ENO and WENO schemes for computational fluid dynamics, in: High-Order Methods for Computational Physics, in: Lecture Notes in Comput. Sci. Eng., vol. 9, Springer, Berlin, 1999, pp. 439–582.
[28] S. Labbé, E. Lorin, On the reservoir technique convergence, submitted for publication.
[29] F. Alouges, G. LeCoq, E. Lorin, Two-dimensional extension of the reservoir technique for linear hyperbolic systems, J. Sci. Comput. 31 (3) (2007).
[30] F. Alouges, B. Merlet, Approximate shock curves for non-conservative hyperbolic systems in one space dimension, J. Hyperbolic Differ. Equ. 4 (2004).